IOPscience iopscience.iop.org

Home Search Collections Journals About Contact us My IOPscience

Formation of vortex clusters and giant vortices in mesoscopic superconducting disks with strong disorder

This article has been downloaded from IOPscience. Please scroll down to see the full text article.

2008 J. Phys.: Conf. Ser. 97 012172

(http://iopscience.iop.org/1742-6596/97/1/012172)

View the table of contents for this issue, or go to the journal homepage for more

Download details:
IP Address: 146.175.13.243
The article was downloaded on 20/05/2010 at 10:43

Please note that terms and conditions apply.

Formation of Vortex Clusters and Giant Vortices in Mesoscopic Superconducting Disks with Strong Disorder

W. Escoffier, I.V. Grigorieva

School of Physics and Astronomy, University of Manchester, Manchester M13 9PL, UK

V.R. Misko[1], **B.J. Baelus, F.M. Peeters**

Department of Physics, University of Antwerpen, Groenenborgerlaan 171, B-2020 Antwerpen, Belgium

L.Y. Vinnikov, S. Dubonos

Institute of Solid State Physics, Russian Academy of Sciences, Chernogolovka 142432, Russia

E-mail: vyacheslav.misko@ua.ac.be

Abstract. Merged, or giant, multi-quanta vortices (GVs) appear in very small superconductors near the superconducting transition due to strong confinement of magnetic flux. Here we present evidence for a new, pinning-related, mechanism for vortex merger. Using Bitter decoration to visualise vortices in small Nb disks, we show that confinement in combination with strong disorder causes individual vortices to merge into clusters/GVs well below T_c and H_{c2}, in contrast to well-defined shells of individual vortices found in the absence of pinning.

1. Introduction

Mesoscopic superconductors exhibit complex and unique vortex structures due to the competition between surface superconductivity and vortex-vortex interactions [1-6]. For mesoscopic disks, theoretical studies found two kinds of superconducting states: a giant vortex (GV), i.e., a circular symmetric state with a fixed value of angular momentum that can carry several flux quanta [1,2] and multivortex states (MVS) with an effective total angular momentum corresponding to the number of vortices in the disk (vorticity L) [3]. Recently, it became possible to experimentally distinguish between a single-core GV and a MVS composed of singly quantized vortices using the multiple-small-tunnel-junction method [4]. GVs have also been inferred from an experimental observation that vortices in perforated Al films merge into large flux spots close to the superconducting transition temperature T_c [7]. In another recent experiment [5], Bitter decoration was used to directly visualise MVS in small Nb disks and circular symmetry was found to lead to the formation of concentric shells of vortices, similar to electron shells in atoms. Analysis of different vortex configurations revealed the

[1] To whom any correspondence should be addressed.

© 2008 IOP Publishing Ltd

rules ("periodic law") of shell filling and also "magic-number" configurations corresponding to commensurability between the shells [6,8].

Here we show that, while weak pinning in mesoscopic disks only leads to distortions in symmetric shell configurations, the presence of strong disorder changes the situation dramatically. Using Bitter decoration to visualise vortices in small disks etched in the surface of Nb single crystals and numerical simulations to analyse the role of disorder, we found [9] that the interplay between confinement and pinning results in the formation of clusters or even GVs in relatively large samples and at temperatures well below T_c, due to *selective enhancement* of pinning strength by disks' boundaries. Depending on the disk's size and the applied field, either all vortices merge into a single cluster/GV (typically for L=3 to 6) or clusters/GVs coexist with singly quantised vortices, for larger L. No clustering /GV formation was found for the same disorder in macroscopic samples.

2. Experimental observation of clustering/GV formation

Samples for this study were prepared from bulk Nb single crystals using e-beam lithography and reactive etching (CF_4 with added oxygen) followed by high-vacuum annealing (at $<10^{-8}$ torr) at temperatures ~ 750ºC, to remove gaseous contaminants. This produced large arrays of disks - 0.5 to 1.4 μm high, of 2 to 5μm diameters - on the surface of ~ 0.5mm thick Nb crystals (see upper-right inset in Fig. 1a). The array geometry and decoration details were the same as in [5], i.e., a whole array of over 300 disks was decorated in each experiment after field cooling to ~1.8K, allowing us to obtain simultaneous snapshots of up to a hundred vortex configurations in nominally identical disks. To assess the degree of disorder before and after annealing, the samples were decorated straight after etching, and then after annealing for t = 1, 2, 4 and 6 hours, and magnetisation and resistivity were measured at t>2h. This revealed pronounced changes in T_c and bulk pinning, consistent with the presence of solute oxygen atoms in interstitial positions [10,11]. By varying the annealing time we were able to achieve partial removal of solute oxygen thereby changing the degree of disorder (for details, see [9]). Accordingly, no vortices were observed either in the bulk of the crystals or inside the disks for t < 2h, as contamination rendered the samples non-superconducting at relevant T, but annealing for $t \geq$ 2h recovered superconductivity over the entire crystals, with the amount of disorder gradually decreasing with increasing t – see Fig. 1*b,c*. The disordered and very inhomogeneous vortex distribution in Fig. 1*b* is consistent with the presence of many pins with sizes $\geq\xi$ [12]. Longer t resulted in a homogeneous, although still disordered, vortex structure (Fig. 1*c*), very similar to that in macroscopic Nb films from our previous study [5].

Fig. 1a (bottom-right inset) shows a typical vortex configuration in disks with weak disorder. Clearly, the effect of vortex confinement in single-crystal-based disks is very similar to that in individual thin-film disks studied in [5], i.e., confinement has a mitigating effect on disorder in that, despite the presence of weak pinning, vortices form nearly perfect shell configurations [e.g., state (1,6,13) in Fig. 1*a*]. Furthermore, both systems show identical diamagnetic response (see Φ/Φ_0 vs L curves in Fig. 1*a*, where $\Phi = H \cdot S$ is the flux through the disk's area S, H the applied magnetic field and Φ_0 the flux quantum), same vortex shell states are observed over corresponding intervals of Φ/Φ_0, etc. Details of the observed behavior will be published elsewhere. The only important implication for the present study is that the effect of vortex confinement in single-crystal-based disks is identical to that in individual thin-film disks, even though in the former case only a small fraction of the total vortex length is subject to the additional interaction with the surface. Moreover, the response was found to be independent of the disk's height, in agreement with theoretical predictions [13]. In contrast, in the case of strong disorder (as in Fig. 1*b*), instead of mitigating pinning as above, confinement was found to *selectively enhance* the effect of pins, ultimately leading to merger of vortices into clusters/GVs, as demonstrated below. The most striking features of vortex configurations in this case are, firstly, that some of the "vortices" inside the disks appear to be *significantly larger* than vortices in the bulk or in weak-disorder disks and, secondly, that there are on average noticeably *fewer* vortices in these disks, compared to the number expected for a given value of Φ/Φ_0 or found in weak-disorder samples, i.e., they show a stronger diamagnetic response and a significant variation in the observed value of L for

the same Φ/Φ_0, as demonstrated in the main panel of Fig. 1*a*. Indeed, a wide range of L values is observed for any given Φ/Φ_0 (e.g. L = 2-6, 8, and 9 for Φ/Φ_0 = 17-19 while only L = 12 and 13 are found for this flux interval in weak-disorder disks) and even the maximum observed L is 25-30% lower than for the weak-pinning disks, indicating that strong disorder somehow facilitates expulsion of extra vortices. The two left insets of Fig. 1*a* show vortex images observed in the same experiment (H = 70 Oe) in identical 3μm disks. Vortices in the bottom image form a slightly distorted shell configuration (1,7) while a disordered pattern of only 5 vortices is seen in the second disk of exactly the same area, with one of the vortices having a ~ 2.5 times larger diameter compared to the rest. Indeed, identifiable shell configurations containing identical (small) vortices were seen only rarely in

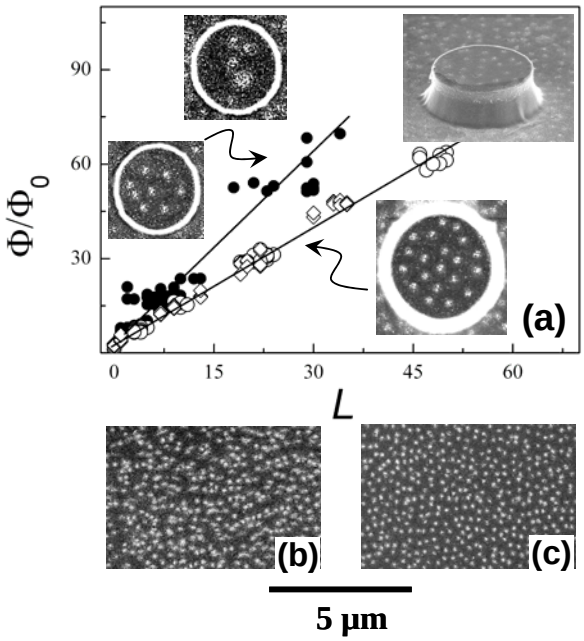

Figure 1. (a) Main panel: Diamagnetic response of single-crystal-based disks with weak (○) and strong (●) disorder; data for individual thin-film disks from Ref. [5] included for comparison (◇). Solid lines are guides to the eye. Top-left and bottom-right insets show vortex configurations in disks with strong and weak disorder, respectively (H = 70 Oe). Top-right inset: vortices in and around a 1.4μm high disk decorated after field-cooling in H = 60 Oe. (b,c) Vortex distributions in the bulk of Nb crystals with strong and weak disorder, respectively (*After Ref.* [9]).

these samples while most disks contained a combination of small and large vortices in a disordered pattern or just a single large vortex. Fig. 2 shows typical observations for 2, 3 and 5 μm disks at Φ/Φ_0 corresponding to different L_{max} (i.e., maximum number of vortices found in disks with only small, singly-quantized, vortices). For L_{max}=3 most disks contained 2 or 3 standard-size vortices (top image), i.e., the diameter of a cluster of Fe particles 'decorating' a vortex was the same as for vortices in the bulk and in weak-disorder disks, but a significant proportion of disks showed only one vortex of about 80% larger diameter (bottom image). For L_{max} = 9 only 10% of the disks showed configurations of small vortices (top image) while most of the rest contained a combination of several small and 1 or 2 large vortices (as in bottom image) and a few disks showed only one very large vortex, as in the bottom image for L_{max} = 11. As the vorticity increased above L_{max} = 11, very few disks contained only small vortices while a typical configuration was a combination of small vortices and a number of large vortices of several different diameters, as in the image for L_{max} = 36.

3. Numerical simulations and discussion

To understand the nature of large vortices observed in disks with strong disorder, we recall that there is an excellent correlation between the size of vortex images in decoration experiments and the 'magnetic' size of individual vortices, $\propto\lambda$ [14]. This allows us to identify the observed large vortices as several singly quantized vortices merged into GVs or clusters with vorticity $L^* \geq 2$ (as explained below, Bitter decoration does not allow us to distinguish between a single-core GV and a multi-core cluster). We emphasise that, although the presence of strong disorder appears to be the necessary condition for the formation of GVs/clusters, they are only formed in small disks and were never observed in the bulk of the same crystals (away from the disk arrays). To estimate L^* associated with different clusters/GVs we analysed intensity profiles of many different vortex images [9]. We distinguish between the results obtained on disks containing only individual, only merged, or a

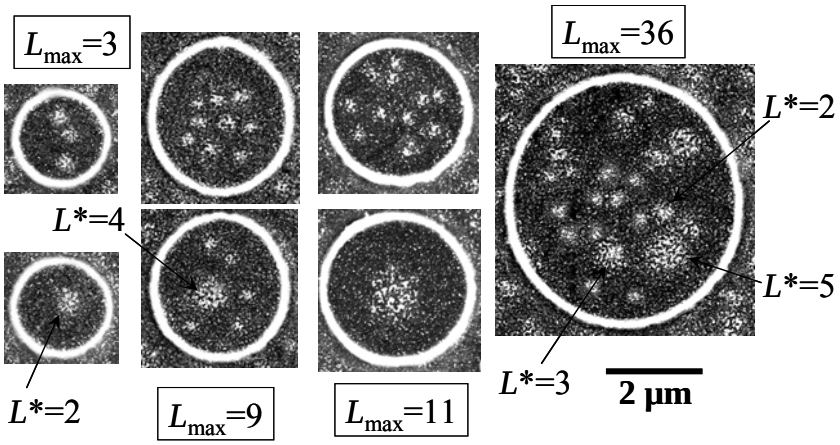

Figure 2. Vortex configurations in disks with strong disorder for different values of L_{max} (see text). L^* is the vorticity of GVs/clusters estimated from their diameters (*After Ref.* [9]).

combination of individual and merged vortices: (i) the size of individual vortices is well defined and shows only small variations between different disks and/or the bulk; (ii) merged vortices show only few typical sizes (rather than a continuous distribution), with the same sizes found in disks with only one merged vortex (where the vorticity can be determined fairly unambiguously from L vs Φ/Φ_0 curves) and in disks containing combinations of individual and merged vortices. This allowed us to identify the number of vortices merged in different clusters/GVs, L^* [9].

To model the role of pinning in a confined geometry theoretically, we place a superconducting disk of thickness d and radius R in a perpendicular external field $\boldsymbol{H}$. The forces of vortex interactions with each other $\mathbf{f}_i^{vv}$ and with the shielding currents and the edge $\mathbf{f}_i^{s}$ can then be modelled as [14,15] $\mathbf{f}_i^{vv} = f_0\Sigma_{i,k=1,L}\{(\mathbf{r}_i - \mathbf{r}_k)/|\mathbf{r}_i - \mathbf{r}_k| - r_k^2(r_k^2\mathbf{r}_i - \mathbf{r}_k)/|r_k^2\mathbf{r}_i - \mathbf{r}_k|\}$ and $\mathbf{f}_i^{s} = f_0\{1/(1 - r_i^2) - h\}\mathbf{r}_i$, where $h = \pi R^2\mu_0 H/\Phi_0 = (H/2H_{c2})(R/\xi)^2$, $\mathbf{r}_i = \boldsymbol{\rho}_i/R$ is the position of the ith vortex, L the vorticity, and $f_0 = 4\pi\mu_0\xi^2H_c^2/R$ the unit of force. Our numerical approach is based on the Langevin dynamics algorithm. Then the overdamped equations of motion become: $\eta\mathbf{v}_i = \mathbf{f}_i = \mathbf{f}_i^{vv} + \mathbf{f}_i^{vp} + \mathbf{f}_i^{T} + \mathbf{f}_i^{s}$. Here $\mathbf{f}_i^{vp}$ is the force due to vortex-pin interactions (see, e.g., [16,17]) which is modelled by short-range parabolic potential wells located at positions $\mathbf{r}_k^{(p)}$; η is the viscous Bardeen-Stephen friction, which we take $\eta = 1$. The pinning force is $\mathbf{f}_i^{vp} = \Sigma_{k=1,Np}(f_p/r_p)|\mathbf{r}_i - \mathbf{r}_k^{(p)}|\,\Theta(r_p - |\mathbf{r}_i - \mathbf{r}_k^{(p)}|\,\mathbf{r}_k)\,\mathbf{r}_{ik}^{(p)}$, where N_p is the number of pinning sites, f_p the maximum pinning force for each potential well, r_p the pinning range (for a strong disorder some pinning centres can overlap forming a complex potential energy profile), Θ the Heaviside step function, and $\mathbf{r}_{ik}^{(p)} = (\mathbf{r}_i - \mathbf{r}_k^{(p)})/|\mathbf{r}_i - \mathbf{r}_k^{(p)}|$. The $\mathbf{f}_i^{T}$ is the thermal stochastic force satisfying: $\langle \mathbf{f}_i^{T}(t) \rangle = 0$ and $\langle \mathbf{f}_i^{T}(t)\,\mathbf{f}_j^{T}(t') \rangle = 2\eta\delta_{i,j}\delta(t - t')k_B T$. The ground state of the system is obtained by simulating field-cooled experiments.

We now consider a disk containing, e.g., 8 vortices in a field h = 15 (for R =1.5μm, this corresponds to $H \approx$ 45Oe). For a perfect disk (no pinning), vortices form a symmetric two-shell configuration (1,7) (cf. [5]) as shown in Fig. 3*a*. A weak pinning site placed near the disk's centre distorts the symmetric configuration, moving away the central vortex; the rest of the vortices adjust themselves accordingly (Fig. 3*b*). However, the situation changes dramatically if f_p is increased: (i) a stronger pin traps 3 out of 8 vortices resulting in *vortex merger* into a cluster with L = 3 coexisting with individual vortices (Fig. 3*c*), similar to the experimental pattern shown in Fig. 3. A stronger still

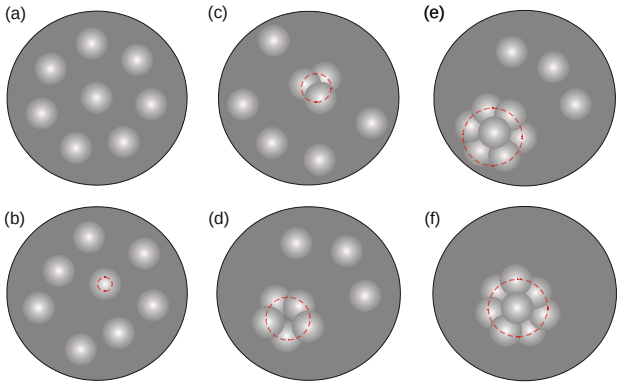

Figure 3. Vortex patterns for L = 8 (a-d) and L = 10 (e,f) in mesoscopic superconducting disks for different pinning potentials: (a) no pinning, perfect (1,7) state; (b) weak pinning, f_p/f_0 = 2, r_p = 0.08, distorted (1,7) state; the range of the pinning potential is shown by red dashed line; (c,d) strong pinning, f_p/f_0 = 4, r_p = 0.16 and f_p/f_0 = 6, r_p = 0.24, respectively; combination of merged and individual vortices; the latter are repelled by the cluster stronger than by a single vortex; (e,f) f_p/f_0 = 8, r_p = 0.32: (e) the pinning site close to the boundary; combination of merged vortices with L=7 and L=3 individual vortices; (f) *enhancement* of the pinning strength of a pinning site near the centre: L=8 vortices are merged, while other vortices are *expelled* from the disk by strong repulsion from the cluster.

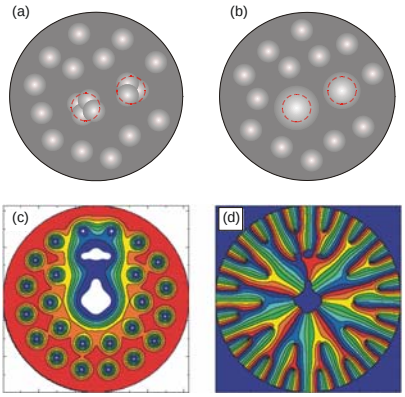

Figure 4. (a,b) Vortex patterns for L = 20; formation of multiquanta vortices in disks with f_p/f_0 = 10, r_p = 0.16 and different r_{min}: (a) r_{min} = 0.048, vortices form clusters with L = 5 (near centre) and L = 4 (out-of-centre); (b) r_{min} = 0.064, GVs with L = 5 (near centre) and L = 4 (out-of-centre); (c) the Cooper pair density, $|\Psi|^2$, in a disk with R = 20ξ, for H=0.2H_{c2}, for two pinning sites with U_0 = 1, and w = 5ξ,; (d) the phase pattern, corresponding to (c), showing a GV with L = 5and a cluster with L = 3.

pin traps 5 out of 8 vortices (Fig. 3*d*). Furthermore, we find that the ability of a pin to trap vortices depends on its *position* inside a mesoscopic disk: a pin close to the disk's centre traps more vortices than the same pin near the boundary (see Fig. 3*e,f*), i.e., its pinning strength is *enhanced* when it is near the centre. (ii) The total vorticity L in a disk with strong pins is *lower* than in the weak-pinning situation because vortices are repelled by a cluster stronger than by a single vortex, pushing them towards the disk boundary so that some vortices leave the sample. This explains the observed *enhanced diamagnetic response* of strong-disorder disks (see Fig. 1). To clarify whether the above vortex merger corresponds to the formation of true GVs with a single core or multiquanta vortex clusters, we calculated the distributions of the order parameter, $|\Psi|^2$, and the phase, ϕ, using the Ginzburg-Landau (GL) equations. It is known [3,4] that in perfect disks without pinning GVs appear as a ground state only if the disk's radius is small enough. For the disk sizes studied here, the ground state in the absence of pinning corresponds to vortex shells (MVS) as observed in Ref. [5]. However, if vortices are trapped by a strong potential they can merge, forming a GV, because repulsive vortex-vortex interaction (logarithmic at small distances [18]) vanishes at very small distances r_{min} when

vortex cores strongly overlap [19]. To demonstrate formation of GVs in disks with strong pinning, we introduced a pinning potential $U_{pin}(\rho)$ in the dimensionless GL equations (see, e.g., [17]): $(-i\nabla - \mathbf{A})^2 \Psi = \Psi [1 - U_{pin}(\rho) - |\Psi|^2]$, where $U_{pin} = U_0 \exp(-\rho/w)$, and $\rho = \sqrt{\{(x-x_{displ})^2 - (y-y_{displ})^2\}}$. The results of calculations of $|\Psi|^2$ and ϕ are shown in Fig. 4*a,b* for a disk with $R = 20\xi$ and pins with $U_0 = 1$ and $w = 5\xi$ at the centre and out-of-centre, respectively. The Cooper pair density $|\Psi|^2$ vanishes at pin positions, forming large spots (larger than individual vortices): The central spot is a GV with vorticity $L = 5$, while the one at the distance of a half of disk's radius is a *cluster* consisting of $L = 3$ individual vortices. Thus, depending on the pinning strength, range and r_{min} (e.g., $r_{min} > 50$ nm for disks with $R = 1$ μm, $f_p/f_0 = 10$, $r_p = 0.16$, as shown in Fig. 4*a,b*, where the lengths are in units of R), vortices can form either clusters (Fig. 4*a*) or GVs with $L = 5$ (centre) and $L = 4$ (out-of-centre), Fig. 4*a*. We note that the above pinning forces are of the same order of magnitude as f_p estimated for normal inclusions in Nb [20] with size $\geq\xi$, with largest pins (>100nm) having f_p and r_p sufficient to form a true GV.

4. Conclusions

We present the first direct observation of pinning-induced merger of vortices in small superconducting disks with strong disorder. The interplay between confinement and disorder is shown to result in the *enhancement* of pinning so that up to 8 vortices can merge into a single cluster or even a GV, which can coexist with individual vortices.

Acknowledgments

This work was supported by the Flemish Science Foundation (FWO-Vl) and the Interuniversity Attraction Poles (IAP) Programme – Belgian State – Belgian Science Policy. V.R.M. is funded by the EU Marie Curie project, Contract No. MIF1-CT-2006-040816.

References

[1] Schweigert V A and Peeters F M 1998 *Phys. Rev.* B **57** 13817
[2] Deo P S, Schweigert V A, Peeters F M and Geim A K 1997 *Phys. Rev. Lett.* **79** 4653
[3] Schweigert V A, Peeters F M and Deo P S 1998 *Phys. Rev. Lett.* **81** 2783
[4] Kanda A, Baelus B J, Peeters F M, Kadowaki K and Ootuka Y 2004 *Phys. Rev. Lett.* **93** 257002.
[5] Grigorieva I V, Escoffier W, Richardson J, Vinnikov L Y, Dubonos S and Oboznov V 2006 *Phys. Rev. Lett.* **96** 077005
[6] Schweigert V A and Peeters F M 1995 *Phys. Rev.* B **51** 770
[7] Veauvy C, Hasselbach K and Mailly D 2004 *Phys. Rev. B* **70** 214513
[8] Misko V R, Xu B and Peeters F M 2007 *Phys. Rev.* B **76** 024516
[9] Escoffier W, Grigorieva I V, Misko V R, Baelus B J, Peeters F M, Vinnikov L Y and Dubonos S and Oboznov V 2007 *Phys. Rev. Lett.* **99** in press
[10] DeSorbo W 1963 *Phys. Rev.* **132** 107
[11] Norman N 1962 *J. Less-Common Metals* **4** 52
Safa H, Moffat D, Bonin B and Koechlin F 1996 *J. Alloys and Compounds* **232** 281
[12] Grigorieva I V 1994 *Supercond. Sci. Technol.* **7** 161
[13] Bezryadin A, Ovchinnikov Y N and Pannetier B 1996 *Phys. Rev. B* **53** 8553
[14] Buzdin A I and Brison J P 1994 *Phys. Lett.* A **196** 267
[15] Baelus B J, Cabral L R E and Peeters F M 2004 *Phys. Rev.* B **69** 064506
[16] Reichhardt C, Olson C J and Nori F 1997 *Phys. Rev. Lett.* **78** 2648
Reichhardt C, Olson C J and Nori F 1998 *Phys. Rev.* B **57** 7937
Reichhardt C, Olson C J and Nori F 1998 *Phys. Rev.* B **58** 6534
[17] Misko V, Savel'ev S, Nori F 2005 *Phys. Rev. Lett.* **95** 177007
Misko V R, Savel'ev S, Nori F 2006 *Phys. Rev.* B **74** 024522
[18] Tinkham M 1996 *Introduction to superconductivity* (New York: McGraw-Hill)
[19] Brandt E-H 1983 *J. Low Temp. Phys.* **53** 41
[20] Campbell A M and Evetts J E 1972 *Adv. Phys.* **21** 199